Basic Design of REBCO Insert Coil of 33 T Cryogen-Free Superconducting Magnet

T. Uto, T. Tosaka, T. Shitaka, H. Nezuka, S. Hanai, H. Takewa, J. Inagaki, S. Ioka, A. Badel, K. Takahashi, et al.

Basic Design of REBCO Insert Coil of 33 T Cryogen-Free Superconducting Magnet

T. Uto, T. Tosaka, T. Shitaka, H. Nezuka, S. Hanai, H. Takewa, J. Inagaki, S. Ioka, A. Badel, K. Takahashi, A. Zampa, T. Okada, Y. Tsuchiya, and S. Awaji

***Abstract*—A 33 T cryogen-free superconducting magnet (33 T-CSM) is under development. The 33 T-CSM consists of a REBCO insert coil and Nb_3Sn/NbTi outsert coils. The REBCO insert coil is designed to generate 19 T in the external field of 14 T. The REBCO insert coil is composed of stacked 64 single pancake coils wound with two bundled REBCO tapes. The inner and outer diameters of the REBCO insert coil are 68 mm and 295 mm, respectively. The REBCO coil is impregnated with epoxy resin for conduction cooling. To prevent delamination of the superconducting layer by thermal stress, the fluorine-coated polyimide tape is co-wound with REBCO tapes and to prevent degradation of superconductivity by electromagnetic stress, reinforcing tape is also co-wound. According to 2D-FEM, it is shown that the circumferential strain ε_θ under applying electromagnetic force is 0.29% . The results of 2D-FEM also suggest that stress concentration occurs at the connection between the coil and the bus bar, and at the widthwise end of the REBCO tape. In this paper, the basic design of the insert coil and the results of FEM analysis will be described.**

***Index Terms*—Cryogen-free, FEM, high field superconducting magnet, insert coil, REBCO coil.**

I. Introduction

In recent years, the development of direct current high magnetic field superconducting magnets has been remarkable. In 2016, a 25 T Cryogen-free Superconducting Magnet (25 T-CSM), combining a Bi-based high temperature superconducting insert coil and Nb_3Sn/NbTi outsert coils, was developed and installed at Tohoku University [1]. In 2017, a superconducting magnet capable of generating 32 T was developed at NHMFL [2]. This magnet combines a REBCO insert coil and a Nb_3Sn/NbTi outsert coil. These direct current high magnetic field superconducting magnets are important tools for research in high magnetic field environments.

In 2022, we launched a new project aiming for even higher magnetic field of 33 T [3]. In this project, a 33 T Cryogen-free Superconducting Magnet (33 T-CSM), which consists of a 19 T REBCO insert coil and a 14 T Nb_3Sn/NbTi outsert coil, is being developed. In designing magnets, it is necessary to prevent the degradation of REBCO tape due to electromagnetic and thermal stresses, and to provide sufficient cooling capacity. For example, in the 32 T magnet at NHMFL, an alumina-plated stainless-steel tape with both insulation and mechanical reinforcement functions is co-wound with the REBCO tape to reduce hoop strain [4]. To prevent the degradation of REBCO tape due to thermal stress, a dry winding without a resin impregnation is performed, and 4.2 K liquid helium is used for cooling. This structure has been successful in achieving the 32 T magnet, which is now available as one of the world's highest field user magnets. However, this type of structure cannot be directly applied to the cryogen-free magnet we are aiming for in our new project. In a cryogen-free magnet, a medium is required for thermal conduction, so it is necessary to impregnate the coil with resin. However, resin-impregnated coils are easy to be degraded due to thermal stress during cooling [5]. In this paper, the results of our study on the basic structure of the 19 T REBCO insert coil for the 33 T-CSM is described.

II. Design of 19 T REBCO Insert

The 33 T-CSM consists of a REBCO insert coil, three Nb_3Sn coils, and two NbTi coils [6]. The schematic structural image of the six coils is shown in Fig. 1. The REBCO insert coil is made up of 64 stacked pancake coils wound with 4 mm wide REBCO tape. The specifications of the REBCO tape and REBCO insert coil are shown in Tables I and II, respectively. The thickness of the substrate of the REBCO tape is 50 μm, and the thickness of copper stabilization layer is 40 μm/side. A cross-sectional view of the pancake coil is shown in Fig. 2. The bundle structure is adopted, in which two REBCO tapes are wound in parallel. Superconducting layers of both REBCO tapes are arranged towards inner diameter. A reinforcing tape for reducing hoop strain and a fluorine-coated polyimide (FCP) tape for separating turns are co-wound with two REBCO tapes, and a total of four tapes are bundled [6]. Turns per single pancake are

T. Uto, T. Tosaka, T. Shitaka, H. Nezuka, S. Hanai, H. Takewa, J. Inagaki, and S. Ioka are with Toshiba Energy Systems & Solutions Corporation, Yokohama 230-0045, Japan (e-mail: tatsuro1.uto@toshiba.co.jp).

A. Badel is with the High Field Laboratory for Superconducting Materials, Institute for Materials Research, Tohoku University, Sendai 980-8577, Japan, and also with the G2Elab/Néel Institute, University of Grenoble Alpes, 38042 Grenoble, France.

K. Takahashi, A. Zampa, Y. Tsuchiya, and S. Awaji are with the High Field Laboratory for Superconducting Materials, Institute for Materials Research, Tohoku University, Sendai 980-8577, Japan.

T. Okada was with the High Field Laboratory for Superconducting Materials, Institute for Materials Research, Tohoku University, Sendai 980-8577, Japan. He is now with the Department of Materials Science and Engineering, Kyushu Institute of Technology, Kitakyushu 804-8550, Japan.

Color versions of one or more figures in this article are available at https://doi.org/10.1109/TASC.2024.3524490.

Digital Object Identifier 10.1109/TASC.2024.3524490

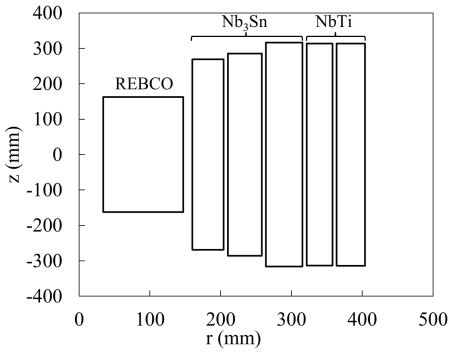

Fig. 1. Schematic composition of 33 T-CSM.

TABLE I
SPECIFICATIONS OF REBCO TAPE

Parameters	Value
Conductor	EuBCO + BHO
Tape width	4 mm
Tape thickness	0.15 mm
Stabilizer	Copper
Stabilizer thickness	40 μm/side
Substrate	Ni-based alloy
Ic at 77K, self-field	>120 A

TABLE II
SPECIFICATIONS OF REBCO INSERT COIL

Parameters	Value
Conductor width	4.1 mm
Conductor thickness	0.15 mm
Number of bundles	2
Thickness of reinforcing tape	0.1mm
Thickness of insulation tape	55 μm
Inner diameter	68 mm
Outer diameter	295 mm
Height	324.8 mm
Turns per SP	247
Number of pancakes	64
Total tape length	18 km
Operating current	358 A

expected to be 247 but it may vary somewhat due to variations in tape thickness.

An over-bind reinforcement is known to suppress the radial expansion of a coil by binding a reinforcing material from the outside of the coil, but it is not very effective for our coils. This is because a soft polyimide tape is placed between the turns, so the restraining force on the outer surface does not reach the tapes which are far from the outer surface. The coil is impregnated with epoxy resin for conduction-cooling, and FRP sheets and high-purity aluminum sheets are attached to the side of the coil. If there is a gap between the pancake coils, the gap will be compressed when subjected to electromagnetic force, causing coils to deform significantly in the axial direction and putting a load on the connecting plate between pancake coils. To prevent deformation of the coils, the gaps between pancake coils are filled with epoxy resin. Epoxy resin fills the gaps between two REBCO tapes, but during winding, some of the resin between the

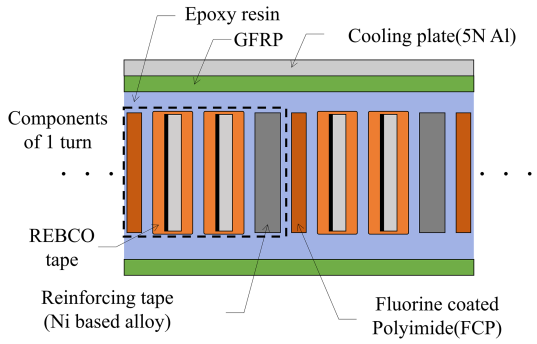

Fig. 2. Schematic drawing of cross section of a pancake coil.

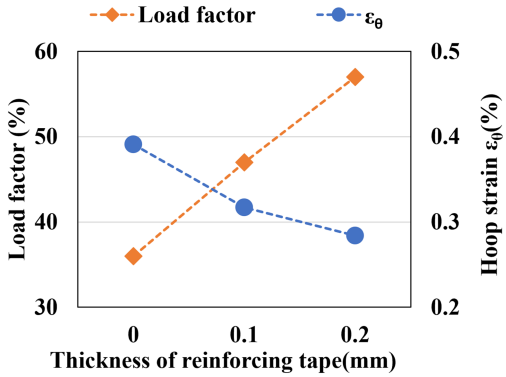

Fig. 3. Dependence of load factor at 15 K and hoop strain in the REBCO insert coil on the thickness of reinforcing tape.

REBCO tapes is pushed out due to tension, causing the bundled REBCO tapes to come into direct contact. As a result, the two bundled REBCO tapes are electrically connected.

The reinforcing tape is made of the same material as the substrate of REBCO tape, nickel-based alloy. The thickness of the reinforcing tape is a design parameter. The thicker reinforcing tape, the more it reduces hoop strain, but the operation current must increase to meet the target current density, and the current load factor becomes higher. Dependence of maximum load factor at 15 K and maximum hoop strain in the REBCO insert on the thickness of reinforcing tape is shown in Fig. 3. The hoop stress is calculated assuming a generalized plane strain state and axial symmetry [7]. The load factors at 15 K for reinforcement wire thicknesses of 0 mm, 0.1 mm, and 0.2 mm are 36% , 47% , and 57% , respectively. Those are 50% , 65% , and 79% , respectively at 20 K. Considering the balance between load factor and hoop strain, we selected 0.1 mm as the thickness of the reinforcing tape and set the operating temperature of the coil to 15 K.

III. 2D-FEM ANALYSIS

A. Analysis Model and Conditions

A 2D-FEM analysis was performed to confirm the stress and strain distribution inside the REBCO insert coil in detail. The analysis model and physical properties of each material are shown in Fig. 4 and Table III, respectively. Axial symmetry and top-bottom symmetry are assumed. The 1st to 3rd, 16th,

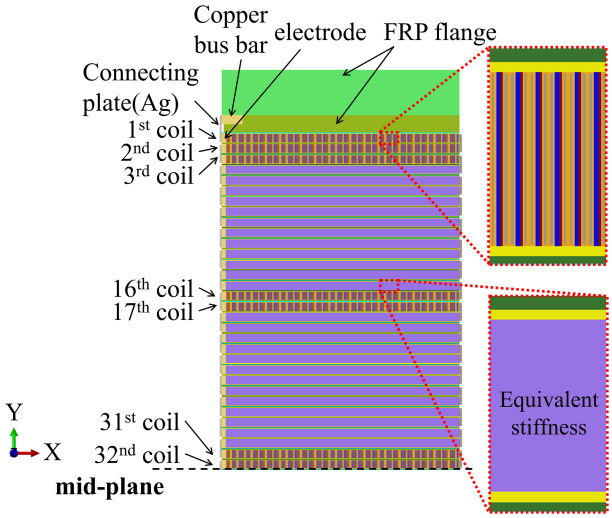

Fig. 4. 2D-FEM model of REBCO insert.

TABLE III
PHYSICAL PROPERTIES OF EACH MATERIAL

	Young's Modulus [GPa]	Poisson's ratio	Thermal shrinkage rate (293 K to 4.2 K)
Cu stabilizer	77	0.34	-0.32
Substrate	215	0.31	-0.22
Ag	83	0.38	-0.43
FRP (warp)	36	0.14	-0.24
FRP (Normal)	21	0.14	-0.71

17th, 31st, and 32nd pancakes from the axial end are modeled in detail: each wire of the winding part is individually modeled. The REBCO tape is modeled by dividing into a copper stabilization layer and a substrate. The REBCO layer and silver stabilizer layer are thin and do not serve as structural members, so they are not modeled. The resin layer between the tapes is too thin to model, so it is estimated to be 5 μm per turn and modeled as a total insulation layer of 60 μm together with the 55 μm thick FCP. Other pancakes are modeled roughly: the winding parts are modeled as the single homogeneous material (equivalent stiffness model). The contact surface is set on both sides of the fluorine-coated polyimide tape to simulate turn-to-turn separation. The analysis consists of three steps: in the step 1, a preload of 0.8 MPa is applied on the coils, in the step 2, the coils are cooled from 293 K to 4.2 K, and in the step 3, electromagnetic stress equivalent to 19 T generation under a background field of 14 T is applied. In this 2D-FEM, it is assumed that the HTS insert coil and LTS outsert coils are charged simultaneously, and the charging delay and shielding current are not considered.

B. Deformation Diagram

The deformation diagram of the entire REBCO insert coil when electromagnetic force is applied is shown in Fig. 5. The contour in Fig. 5 is the von Mises stress. The displacement of the coil is continuous, and there is no significant difference between the detailed model and the equivalent stiffness model.

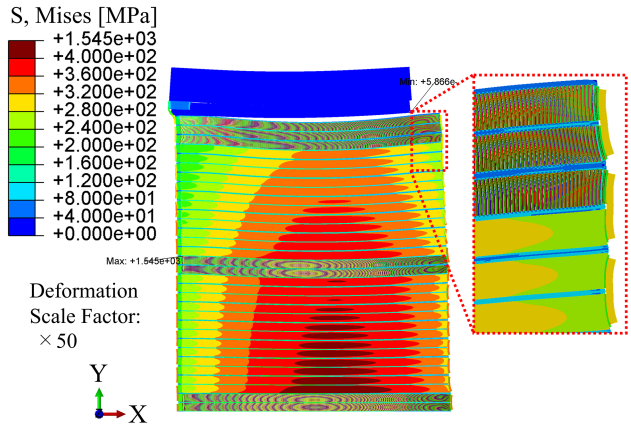

Fig. 5. Deformation diagram of REBCO insert.

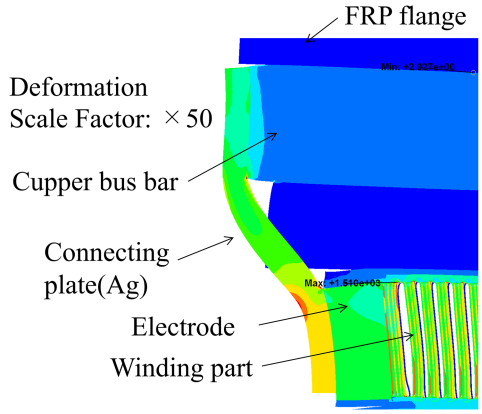

Fig. 6. The enlarged view of the deformation diagram around the connecting plate.

The winding section expands outward due to electromagnetic force, while the copper bus bar is fixed to the FRP flange that does not experience electromagnetic force, causing the connecting plate connecting them to deform into a U-shape. An enlarged view of the deformation around the connecting plate is shown in Fig. 6. Although the connecting plate is significantly deformed, the deformation of the winding part is suppressed by the high-strength inner electrode. In addition, since the plasticity of silver is not considered in this analysis, the actual coil may not generate as much stress as suggested by the analysis.

C. Distribution of Stress and Strain in the Coils

The maximum value of hoop strain generated in the coil was confirmed. Fig. 7 shows the radial distribution of the circumferential strain ε_θ in the 32nd pancake, where the hoop stress is the largest. The data extraction points in Fig. 7 are shown in Fig. 8. Strain data are extracted from the positions of the red circles arranged in a straight line, indicated as Row A/B in Fig. 8. This point is a node separated by one element from the Cu plating boundary of each REBCO tape into the substrate, and the stress/strain at this point is assumed to be the same magnitude as the stress/strain generated in the superconducting layer. The radial distribution of the circumferential strain ε_θ shows a mountain-shaped distribution with a maximum at a

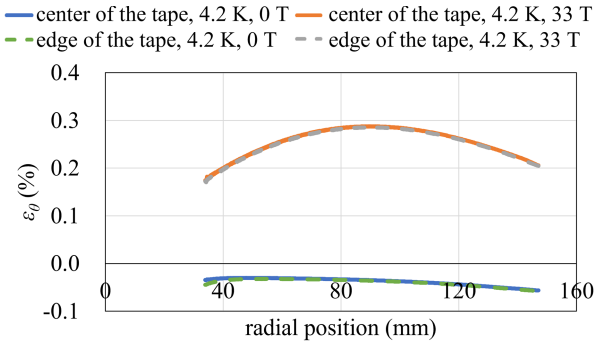

Fig. 7. The radial distribution of circumferential strain ε_θ.

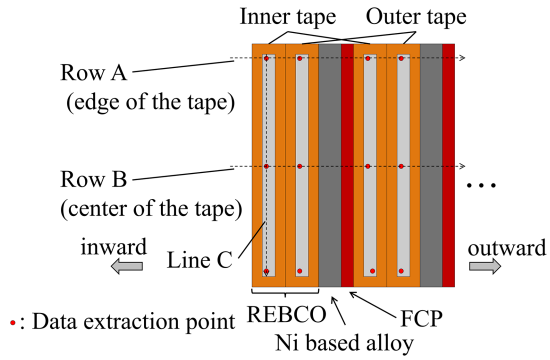

Fig. 8. Data extraction point of Figs. 7, 9 and 10.

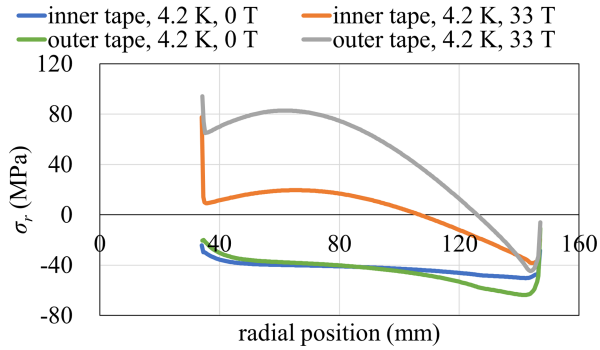

Fig. 9. The radial distribution of radial stress σ_r.

radial position of 90 mm. The thermal strain after coil cooling is -0.036% and the electromagnetic strain is 0.323% . Adding these together, the strain after cooling and charging are 0.287% . The electromagnetic strain of 0.323% is roughly consistent with the value shown in Fig. 3. Fig. 7 suggests that the strain ε_θ at the edge of the tape isn't significantly different from the strain in the center of the tape.

The radial distribution of radial stress is shown in Fig. 9. The stress in Fig. 9 is the value extracted from the position of the red circle along Row A in Fig. 8. Since the stress of the two REBCO tapes have different distributions, they are graphed separately. In Fig. 9, the REBCO tape arranged closer to the inner diameter is labeled as "inner tape", and the REBCO wire arranged closer to the outer diameter is labeled as "outer tape". Radial stress σ_r has a sharp peak near the innermost diameter and shows a mountain-shaped distribution in other area. The stress value

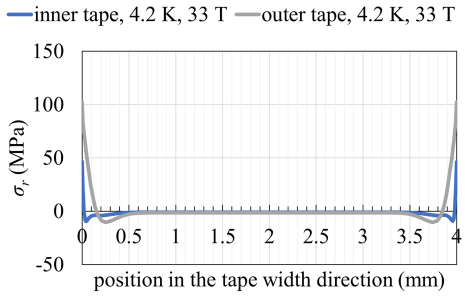

Fig. 10. Radial stress σ_r distribution in the wire width direction at radial position of 60 mm.

at the peak is larger for the outer tape than for the inner tape. This stress works in the direction of delaminating the REBCO layer, which may degrade the superconducting characteristics. The sharp peak near the innermost diameter might be caused by the rigid electrode connected with the REBCO tape. The rigid electrode prevent deformation of the REBCO tape towards the outside and generate stress. In this 2D-FEM, due to circumferential symmetry, it is assumed that there is a ring-shaped copper electrode, but in practice, about two-thirds of the ring is made of copper, and the remaining part is made of FRP. The stiffness of the ring is overestimated, and it is considered that the actual coil does not generate as much stress as suggested by the analysis. There is also a peak with a maximum value of 80 MPa at a radial position of 60 mm. This stress is thought to be due to the difference in elongation between the REBCO tape and the FRP sheet. The pancake coil deforms to increase its outer diameter due to electromagnetic force. The FRP sheet bonded to the side of the pancake coil also deforms to extend in the coil diameter direction. On the other hand, when the REBCO tapes and the integrated reinforcing tapes are subjected to tension in the circumferential direction due to strong hoop stress, the radial dimension of the REBCO tapes is shrunk by the Poisson's ratio. While the FRP sheet becomes larger in the radial direction, the REBCO tape tries to become smaller in the radial direction, so an additional radial stress appears near the interface between the REBCO and the FRP as shown in Fig. 9. The difference in stress between the inner tape and the outer tape can be explained as follows. As shown in Fig. 8, the FCP that separates the turns is arranged adjacent to the inner tape. As a result, the inner surface of the inner tape becomes a free end, so the stress generated is small, while the stress generated on the outer tape, which is far from the free end, is large.

To further investigate this, the distribution of σ_r in the tape width direction of the REBCO tape at a radial position of 60 mm is shown in Fig. 10. The data are extracted along "line C" shown in Fig. 8. σ_r changes in the compression direction at a position 0.2 mm inside from the width end of REBCO layer. This compressive stress may prevent the degradation of REBCO tape characteristics. It is unclear whether the stress concentration is quite a problem or not, so further verification and testing are necessary. In this 2D-FEM, the shielding current is not considered, but in actual high-field magnets, the magnetic strain caused by the shielding current is non-negligible [8], [9]. In future, it is necessary to evaluate the effects of the shielding

current. Although the inner current terminal was investigated here, the detail current terminal structure including an outer current terminal is still under consideration. The final terminal structure will be decided after detail investigations in future.

IV. Conclusion

Basic design of REBCO insert for the 33 T-CSM is presented. The REBCO insert coil generates a 19 T under the background field of 14 T by the LTS outsert coils. The maximum circumferential strain is 0.29% , and the load factor at 15 K is estimated to be 47% . 2D-FEM analysis suggests that there is stress concentration around the connection plate connecting the pancake coil and the copper bus bar, and at the edge of the REBCO tape. To reveal the extent of the risk posed by these stress concentrations, further verification is necessary.

References

[1] S. Awaji et al., "First performance test of a 25 T cryogen-free superconducting magnet," *Superconductor Sci. Technol.*, vol. 30, no. 6, 2017, Art. no. 065001.

[2] "Meet the 32 Tesla Superconducting Magnet," Mar. 21, 2023. [Online]. Available: https://nationalmaglab.org/about-the-maglab/around-the-lab/meet-the-magnets/meet-the-32-tesla-superconducting-magnet/

[3] S. Awaji et al., "Progress of 33 T cryogen-free superconducting magnet," in *Proc. Appl. Supercond. Conf.*, 2024, pp. Sep. 1–6.

[4] A. Voran, H. W. Weijers, W. D. Markiewicz, S. R. Gundlach, J. B. Jarvis, and W. R. Sheppard, "Mechanical support of the NHMFL 32 T superconducting magnet," *IEEE Trans. Appl. Supercond.*, vol. 27, no. 4, Jun. 2017, Art. no. 4300305, doi: 10.1109/TASC.2016.2637163.

[5] H. Miyazaki, S. Iwai, T. Tosaka, K. Tasaki, and Y. Ishii, "Degradation-free impregnated YBCO pancake coils by decreasing radial stress in the windings and method for evaluating delamination strength of YBCO-coated conductors," *IEEE Trans. Appl. Supercond.*, vol. 24, no. 3, Jun. 2014, Art. no. 4600905, doi: 10.1109/TASC.2013.2287054.

[6] S. Awaji et al., "Robust REBCO insert coil for upgrade of 25 T cryogen-free superconducting magnet," *IEEE Trans. Appl. Supercond.*, vol. 31, no. 5, Aug. 2021, Art. no. 4300105, doi: 10.1109/TASC.2021.3061896.

[7] W. D. Markiewicz et al., "Generalized plane strain analysis of superconducting solenoids," *J. Appl. Phys.*, vol. 86, no. 12, pp. 7039–7051, Dec. 1999, doi: 10.1063/1.371791.

[8] D. Kolb-Bond, M. D. Bird, T. Painter, S. K. Ramakrishna, and A. Reyes, "Screening current induced field changes during de-energization with axial clamping," *IEEE Trans. Appl. Supercond.*, vol. 32, no. 6, Sep. 2022, Art. no. 4701404, doi: 10.1109/TASC.2022.3162162.

[9] Y. Yan et al., "Screening-current-induced mechanical strains in REBCO insert coils," *Superconductor Sci. Technol.*, vol. 34, no. 8, Aug. 2021, Art. no. 085012, doi: 10.1088/1361-6668/ac0b2d.